Chapter 6

CELL CULTURE STUDIES

6.1 Introduction

After the preliminary studies of formulation preparation and characterization, the final objective was to deliver these nanoparticulate carriers by parenteral route to animals. But before the animal studies, the formulations should be evaluated for their safety and efficacy at cell culture level. The aim of the study was to evaluate prepared NPs for cancer chemotherapy with a view to explore the possible effects of particle size, conjugation and particle surface coating on the cell uptake. Hence, the cell uptake, cytotoxicity studies, cell cycle analysis and apoptosis studies were taken up prior to in-vivo studies. Cell uptake studies were carried out using 6-Coumarin (lipophilic fluorescent dye) loaded NPs with the aim of finding whether the NPs are internalized into the cells and to determine the intracellular concentrations of the loaded dye.

6.1.1 Cellular uptake

The primary advantage in using macromolecules as drug delivery vehicles is their mechanism of cellular internalization. The cell membrane is naturally impermeable to complexes larger than 1 kDa; however, cells possess a variety of active internalization mechanisms to accommodate cellular entry of large molecular complexes. Here, the cell membrane will invaginate to engulf molecules and extracellular fluid in an intracellular membrane bound vesicle or endosome, which will subsequently travel through the cell, a process known as endocytosis [Castino et al. 2003]. NPs may reside near the membrane or directly interact with membrane proteins to enable their retention in these vesicles. Analogous to the attachment of drug moieties to high molecular weight carriers, agents such as antibodies and high affinity ligands can be surface conjugated in order to exploit direct membrane interactions and target these complexes to specific cell populations in organ systems. Targeting macromolecular complexes with high affinity ligands specific to membrane proteins, namely receptors, can aid in regulating not only the cellular recognition of these carriers but also the trafficking pathway and subcellular localization within the cell [Sly and Vogler 2002].

The major objective for targeted drug delivery includes enhancing drug accumulation at the target site as well as reducing the non-selective uptake of toxic agents. In order to target drugs to specific tissue systems within the body, drug molecules can be directly attached to a targeting agent or complexed with a vehicle, or macromolecule, that contains targeting moieties. Macromolecules can be bioengineered to incorporate a

variety of synthetic and natural compounds including drugs, ligands, and radionuclides [Bareford and Swaan 2007].

6.1.2 Cytotoxicity studies

The MTT (3-(4,5-dimethylthiazole-2-yl)-2,5-diphenyltetrazoliumbromide) and the ATP (adenosine triphosphate) assays are widespread methods to assess cell viability. MTT is reduced by mitochondrial dehydrogenases in living cells to a blue-magenta colored formazan crystals. The absorption of dissolved formazan in the visible region correlates with the number of intact alive cells. Cytotoxic compounds are able to damage and destroy cells, and thus decrease the reduction of MTT to formazan [Mosmann 1983]. One remarkable disadvantage of the MTT assay is that damaged mitochondria may still be able to reduce MTT to formazan [Sieuwerts et al. 1995]. This could lead to a rightward shift of the concentration-response (absorption) curves. Damaged mitochondria could further evolve from sharp formazan crystals/needles and alter the reduction of MTT to formazan. Thus, the formation of cell/mitochondria damaging formazan needles was prevented by microscopic supervision of needle formation and led to an optimized incubation time for MTT of 50-70 min. Furthermore, more than 1 enzyme involved in oxidative/reductive metabolism may play a role in the reduction of MTT to formazan [Loveland et al. 1992]. The development of the MTT assay as a homogeneous assay was, however, a major achievement since washing steps during the MTT assay were associated with the loss of less attached damaged and living cells leading to a higher degree of variation.

6.1.3 Apoptosis

Apoptosis is a process of programmed cell death that may occur in multicellular organisms. Biochemical events lead to characteristic cell changes and death. Cells undergoing apoptosis show characteristic morphological and biochemical features. The characteristics include chromatin aggregation, nuclear and cytoplasmic condensation, while necrosis displays a direct injury to the cell. Determination of cell death mechanism is important to compare effectiveness of NP formulations. Apoptosis study of prepared NPs was conducted using Annexin V staining procedure in MCF7 cell line. This assay takes advantage of the fact that phosphatidylserine (PS) is translocated from the inner (cytoplasmic) leaflet of the plasma membrane to the outer (cell surface) leaflet soon after the induction of apoptosis. Annexin V protein has a strong and specific affinity for PS which can be used as a probe for estimation [Susin et al. 2000].

6.1.4 Cell cycle analysis

Analysis of replication state in a population of cells can be achieved by fluorescence labelling of the nuclei of cells in suspension and then analyzing the fluorescence properties of each cell in the population. The distribution of DNA in the cell replication state was studied by flow cytometry [Panyam and Labhasetwar 2003; Vega et al. 2006]. Quiescent and G1 cells will have one copy of DNA and will therefore have 1× fluorescence intensity.

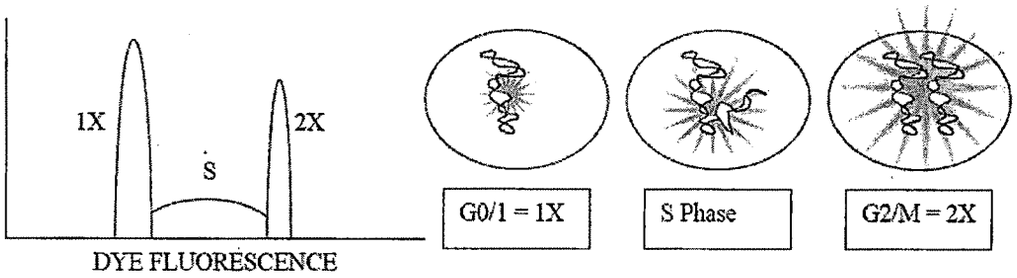

Figure 6.1 Schematic presentation of principle for cell cycle analysis using DNA intercalating florescence probe in flow cytometry.

Cells in G2/M phase of the cell cycle will have two copies of DNA and accordingly will have 2× intensity. Since the cells in S phase are synthesizing DNA they will have fluorescence values between the 1× and 2× populations (figure 6.1). The resulting histogram consists of three populations: two Gaussian curves (1× and 2× peaks) and the S phase population. Adjacent populations overlap each other. Because of this, a modelling program is required to de-convolute the populations and assign percentage values to each population. Expert and subjective review of the modelling software's cell cycle phase percentage assignment is the final stage of cell cycle analysis prior to reporting the results.

6.2 Materials

Sulpho-NHS and 6-Coumarin dye were purchased from Sigma-Aldrich, Mumbai, India. Monoclonal antibody against estrogen receptor was purchased from Pierce antibodies, Rockford, IL, USA. All other chemicals were of analytical reagent grade and obtained commercially. RPMI-1640, MEM, Fetal Bovine Serum (FBS), antibiotic-antimycotic, Trypsin-EDTA and PBS were purchased from Life Technologies India Pvt. Ltd., New Delhi, India. 6-well plates, 96-well plates, tissue culture flask (25 and 75 cm^2), chamber

slide and other sterile material for cell culture were purchased from Thermo scientific, Mumbai, India. Annexin V-FITC apoptosis detection kit was obtained from BD Pharmingen, CA, USA. Hoechst stain was purchased from Invitrogen, Mumbai, India. EDC and NHS were purchased from Himedia, Vadodara, India.

6.3 Cell lines

MCF7 and MDAMB231 cells were procured from NCCS, Pune, India. Estrogen receptor positive, MCF7 cell line, was cultured in MEM medium (Gibco, Grand Island, NY, USA) supplemented with 10% (v/v) FBS. Estrogen receptor negative, MDAMB231 cell line, was cultured in RPMI-1640 medium supplemented with 10% (v/v) FBS. All cell lines were supplemented with penicillin (100 units/ml) and streptomycin (100 µg/ml) (Gibco, Grand Island, NY, USA) at 37 °C in a humidified incubator containing 5% CO_2.

6.4 Methods

6.4.1 Receptor expression analysis by Western Blot

A comparative expression of estrogen receptor in breast cancer cell lines (MCF7 and MDAMB231) was estimated by Western Blot analysis [Van Maerken et al. 2006]. Briefly, 2.5×10^5 cells of different cell lines (MCF7 and MDAMB231) were seeded in culture flask (75 cm^2, Nunc, India) and allowed to reach confluency. Thereafter, the cells were trypsinized and collected by centrifugation. The cells were lysed in lysis buffer (150 mM NaCl, 1% NP-40, 1% sodium deoxycholate, 0.1% SDS, 50 mM Tris-HCL, pH 7.5, 2 mM EDTA) containing 1% protease inhibitor cocktail (Sigma Aldrich, USA) and incubated for 30 min. Subsequently, the lysates were centrifuged (10,000 rpm for 10 min at 4 °C), and the supernatants were used for further analysis. Protein concentration was determined by Bradford's method [Bradford 1976]. Aliquots of each sample containing 60 µg proteins were resolved on a SDS-polyacrylamide gel, by electrophoresis at 40 mA for 2 h and transferred to 0.45 µm polyvinylidene difluoride membranes (Millipore, USA). Membranes were then probed with primary antibodies specific to ER diluted at 1:2000 v/v. The membranes were washed three times with PBS containing 1% tween-80 and probed with goat anti-mouse secondary antibody. Protein bands were detected using chemiluminescence and densitometric analysis was carried out using Quantity one Quantitation software (Bio-Rad, USA).

6.4.2 Qualitative cellular uptake by fluorescent microscopy

5×10^4 MCF7 cells were seeded in chamber slides and allowed to attach and grow. After 48 h, the cells were incubated with 1 ml, 10 µg/ml 6-Coumarin, 6-Coumarin loaded PLGA NPs, 6-Coumarin loaded PCL NPs, pegylated PLGA NPs, pegylated PCL NPs, pegylated PLGA ImmunoNPs and pegylated PCL ImmunoNPs for 2 h. Adhered cells were washed with 1× PBS and treated with 1 ml (1 µg/ml) Hoechst 33342 for 15 min. Cells were again washed with 1× PBS and visualized under fluorescent microscope (Leica, DMLB, Weltzar, Germany) using FITC and DAPI filters.

6.4.3 Quantitative cellular uptake by flow cytometry

1×10^5 MCF7 cells were seeded on 6-well plate and allowed to attach and grow. After 24 h, cells were incubated with 1 ml of medium containing 100 µg/ml 6-Coumarin, 6-Coumarin loaded PLGA NPs, PCL NPs, pegylated PLGA NPs, pegylated PCL NPs, pegylated PLGA ImmunoNPs and pegylated PCL ImmunoNPs for 30, 60 and 90 min. Cells with only medium were used as respective controls. At the end of the incubation period, the cell monolayer was washed three times with cold 1× PBS to eliminate excess of dye or NPs, which were not taken up by the cells and then trypsinized. Cells were collected by centrifugation at 400×g (Eppendorf centrifuge, USA) and analyzed in FACS (FACS Canto-II, BD Biosciences, CA, USA) using software provided with the instrument (BD FACS Diva 6.2.1 software, BD Biosciences, CA, USA) for total amount of NPs uptake by 10,000 cells.

6.4.4 In vitro cytotoxicity studies by MTT Assay

MTT assay was done to evaluate the mitochondrial activity according to the method of Mosmann [Mosmann 1983]. MCF7 cells were seeded in 96-well plate (7000 cells/well) and allowed to attach and grow. After 24 h, the medium was removed and replaced with 100 µl medium containing different concentration of NPs and incubated for different time periods (6, 24, 48 h). After incubation, treatment media was removed and cells were treated with 100 µl (5 mg/ml) of MTT dye [3-(4,5-dimethylthiazoyl-2-yl)-2,5-diphenyltetrazolium bromide] 3 h prior to completion of incubation periods. The medium from each well was discarded and resulting formazan crystals were solubilized in 200 µl of dimethylsulphoxide and quantified by measuring absorbance at 550 nm in multiwell plate reader (SYNERGY-HT, Bio-Tek, Winooski, Vermont, USA) using KC4 software.

6.4.5 In vitro apoptosis study

2×10^5 MCF7 cells were seeded on 6-well plates and allowed to attach and grow for 24 h. Cells were incubated with 2 ml media containing 1 µM ATZ solution, ATZ loaded PLGA NPs, PLGA-PEG NPs, PLGA-PEG ImmunoNPs, PCL NPs, PCL-PEG NPs and PCL-PEG ImmunoNPs for 24 and 48 h. Cells were also incubated with 2 ml media containing 1 µM EXE solution, EXE loaded PLGA NPs, PLGA-PEG NPs, PLGA-PEG ImmunoNPs, PCL NPs, PCL-PEG NPs and PCL-PEG ImmunoNPs for 24 and 48 h. After incubation, cells were harvested and washed. Incubation media, washing buffer and trypsin-EDTA treated cell were collected together and centrifuged at 1,500 rpm for 5 min. Cells were suspended in 100 µl binding buffer and stained with Annexin-FITC (2 µl), mixed well using vortex shaker and incubated at room temperature, protected from light for 15 min. After incubation, propidium iodide (PI, 2 µl, 50 µg/ml) was added and incubated at 4 °C for 10-15 min. After incubation, 200 µl of additional binding buffer was added, and suspension was analyzed using FACS at Texas red and FITC channel (FACS Canto-II, BD Biosciences, CA, USA) using software provided with the instrument (BD FACS Diva 6.2.1 software, BD Biosciences, CA, USA). The intensity plot of FITC vs. Texas Red was sectioned in four quarters to differentiate stained and unstained cells. Based on four quarters, percentage of cells in early apoptotic phase (FITC positive and PI negative), late apoptotic phase (FITC and PI positive) and necrotic phase (FITC negative and PI positive) were recorded.

6.4.6 Cell cycle analysis by flow cytometry

2×10^5 MCF7 cells were seeded on 6-well plate and allowed to attach and grow for 24 h. Cells were incubated with 2 ml media containing 1 µM ATZ solution, ATZ loaded PLGA-PEG NPs, PLGA-PEG ImmunoNPs, PCL-PEG NPs and PCL-PEG ImmunoNPs for 24 h. Cells were also incubated with 2 ml media containing 1 µM EXE solution, EXE loaded PLGA-PEG NPs, PLGA-PEG ImmunoNPs, PCL-PEG NPs and PCL-PEG ImmunoNPs for 24 h. After incubation, medium was aspirated in to individual tubes. Cells were washed with 1× PBS and harvested with 200 µl of trypsin-EDTA, later 500 µl of complete medium was added to quench the trypsin activity. Cells were collected together in to the same tubes where the medium was aspirated earlier and centrifuged at 500×g for 5 min. The cell pellet was washed twice with PBS and centrifuged. Cells were re-suspended in 1 ml ethanol (70%) for fixing and kept at -20 °C for 30 min. Cells were centrifuged and were lysed in 250 µl 1× PBS containing 0.2% triton X 100 and incubated at 4 °C for 30 min.

They were again centrifuged and re-suspended in 500 µl 1× PBS containing 20 µl RNAse (10 mg/ml) and incubated at 37 °C for 30 min. Cells were then centrifuged and re-suspended in 500 µl of 1× PBS containing 10 µl propidium iodide (1 mg/ml) and incubated for 10-15 min at 4 °C. Thereafter, cells were analyzed on FACS by recording signal from Texas red channel (FACS Canto-II, BD Biosciences, CA, USA) using software provided with the instrument (BD FACS Diva 6.2.1 software, BD Biosciences, CA, USA). Histogram of count vs. intensity was made to calculate ratio of cells under G0/G1 (2n), S (2n+), G2/M phase (4n) and under apoptosis (2n-).

6.5 Results and discussion

6.5.1 Receptor expression in cell lines

The drug loaded ImmunoNPs were prepared with the objective of receptor mediated endocytosis in ER positive breast tumor cells for preferential accumulation of drug at tumor site. To achieve this, expression levels of ER in breast cancer cell lines, MCF7 and MDAMB231 were assessed by Western Blotting. The results confirmed the expression of ER in MCF7 cell line and absence of this receptor in MDAMB231 cell line (figure 6.2). Thus, MCF7 and MDAMB231 cell line served as positive control and negative control for further experiments, respectively.

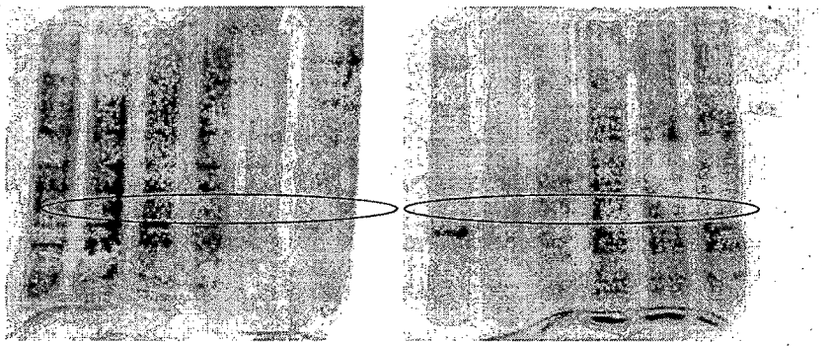

Figure 6.2 Receptor expression analyses in cell lines.

6.5.2 Qualitative and quantitative cellular uptake

Fluorescent property of 6-Coumarin was used for comparative intracellular uptake of NPs in MCF7 cell line by flow cytometry and fluorescent microscopy. The relative extent of PLGA NPs, pegylated PLGA NPs, pegylated PLGA ImmunoNPs, PCL NPs, pegylated PCL NPs and pegylated PCL ImmunoNPs was calculated using mean fluorescent index (MFI) and is shown in figure 6.3, 6.4, 6.5 and 6.6. As evident from figure 6.3, MFI of pegylated

PLGA ImmunoNPs was 1039.10 ± 17.77 which was more than 3 times than that of PLGA NPs (318.27 ± 21.69) after 180 min (table 6.1). Furthermore, pegylated PLGA ImmunoNPs showed about 2 times more uptake when compared with pegylated PLGA NPs (599.95 ± 25.17) at same time point due to receptor mediated endocytosis. As shown from figure 6.5, MFI of pegylated PCL ImmunoNPs is 1261.62 ± 39.27 which is about twice than that of PCL NPs (730.19 ± 38.68) after 180 min (table 6.2). Furthermore, ImmunoNPs showed about 1.32 times more uptake when compared with pegylated PCL NPs (956.45 ± 33.45) at same time point. Intracellular uptake was found to increase with time for all formulations from 60 to 180 min.

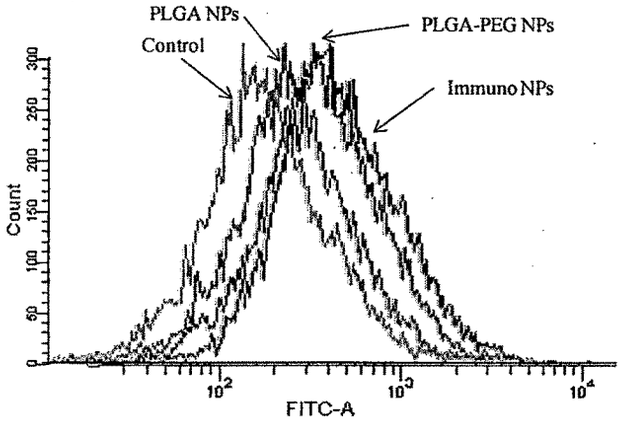

Figure 6.3 Quantitative intracellular uptake histograms of 6-Coumarin loaded PLGA NPs, pegylated PLGA NPs and ER antibody conjugated ImmunoNPs by MCF7 cells using flow cytometry.

The intracellular uptake of NPs was also dependent on the incubation time. The fluorescence intensity increased gradually with the incubation time and so also the uptake of NPs, indicating time dependent uptake. Results clearly indicate the enhanced cellular uptake of ImmunoNPs than un-conjugated systems. Figure 6.4 represents the quantitative uptake study of PLGA NPs, pegylated PLGA NPs and pegylated PLGA NPs by fluorescent microscopy. Figure 6.6 represents the quantitative uptake study of PCL NPs, pegylated PCL NPs and ImmunoNPs by fluorescent microscopy. Our results confirmed that NPs showed augmented fluorescence activity which was found to be maximum with cells treated with ImmunoNPs after 2 h of incubation. The images were consistent with those presented in the flow cytometry analysis as shown in figure 6.7 and 6.8.

The enhanced therapeutic activity of the ImmunoNPs assessed in terms of cellular uptake efficiency of the carrier system clearly demonstrated that uptake of ImmunoNPs

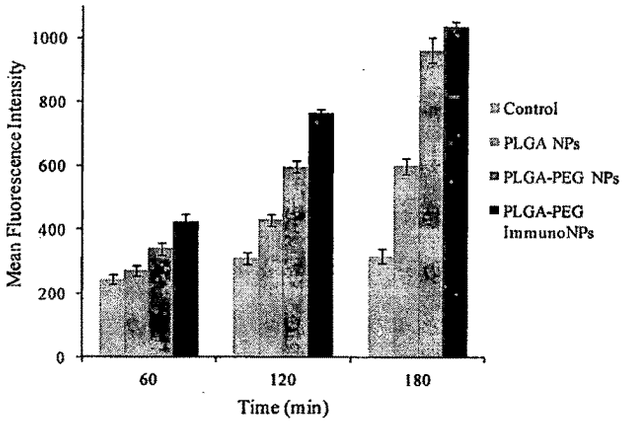

Figure 6.4 Quantitative intracellular uptake of 6-Coumarin loaded PLGA NPs, pegylated PLGA NPs and ER antibody conjugated ImmunoNPs by MCF7 cells using flow cytometry. Uptake was calculated by measuring MFI and represented as mean ± S.D. (n=3)

Table 6.1 Intracellular uptake of 6-Coumarin loaded PLGA NPs, pegylated PLGA NPs and ER antibody conjugated ImmunoNPs by MCF7 cells using flow cytometry. Uptake was calculated by measuring MFI and represented as mean ± S.D. (n=3)

Treatment	Mean Fluorescence Intensity		
	60 min	120 min	180 min
Control	243.8 ± 16.1	310.6 ± 20.1	318.3 ± 21.6
PLGA NPs	270.3 ± 16.9	430.6 ± 19.5	599.9 ± 25.2
PLGA-PEG NPs	340.6 ± 18.8	597.8 ± 18.1	965.7 ± 39.0
PLGA-PEG ImmunoNPs	423.9 ± 24.5	765.0 ± 14.3	1039.1 ± 17.8

was significantly greater than that of the un-conjugated particle and non-pegylated formulations. The greater uptake of ImmunoNPs can be explained on the basis of ER expression in cells and specificity of ER receptor mediated binding of ImmunoNPs. Moreover, the enhanced uptake level of ImmunoNPs can be attributed to the lesser exocytosis of the conjugated system than un-conjugated NPs [Sahoo and Labhasetwar 2005]. Together, all these contribute to the greater intracellular retention of ImmunoNPs. Thus, higher cellular uptake observed with ImmunoNPs is attributed to their greater intracellular delivery by receptor mediated endocytosis.

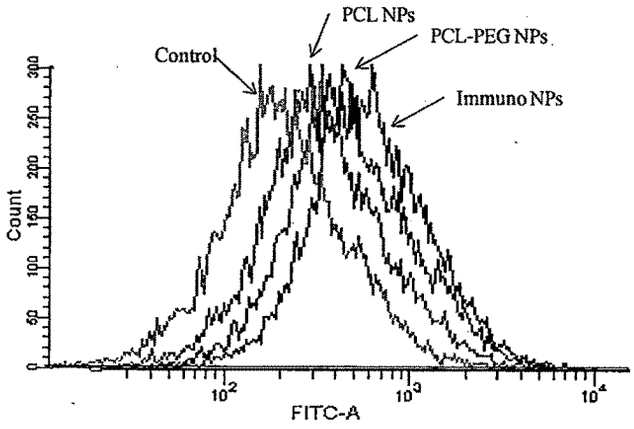

Figure 6.5 Quantitative intracellular uptake histograms of 6-Coumarin loaded PCL NPs, pegylated PCL NPs and ER antibody conjugated ImmunoNPs by MCF7 cells using flow cytometry.

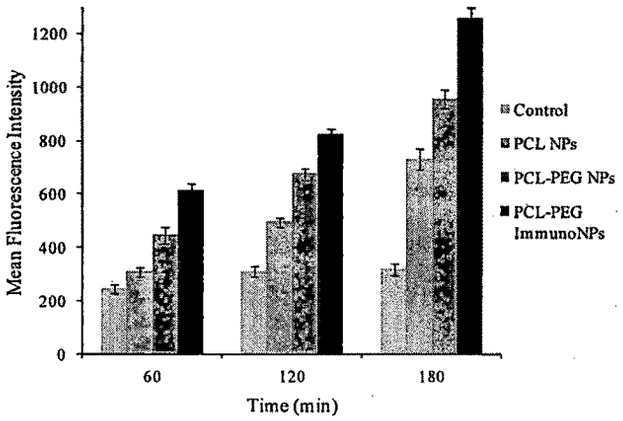

Figure 6.6 Quantitative intracellular uptake of 6-Coumarin loaded PCL NPs, pegylated PCL NPs and ER antibody conjugated ImmunoNPs by MCF7 cells using flow cytometry. Uptake was calculated by measuring MFI and represented as mean ± S.D. (n=3)

Table 6.2 Intracellular uptake of 6-Coumarin loaded PCL NPs, pegylated PCL NPs and ER antibody conjugated ImmunoNPs by MCF7 cells using flow cytometry. Uptake was calculated by measuring MFI and represented as mean ± S.D. (n=3)

Treatment	Mean Fluorescence Intensity		
	60 min	120 min	180 min
Control	243.8 ± 16.1	310.6 ± 20.1	318.3 ± 21.6
PCL NPs	307.1 ± 16.6	493.8 ± 16.4	730.2 ± 38.7
PCL-PEG NPs	446.0 ± 31.2	676.0 ±21.1	956.4 ± 33.5
PCL-PEG ImmunoNPs	613.7 ± 24.6	823.9 ± 19.5	1261.6 ± 39.3

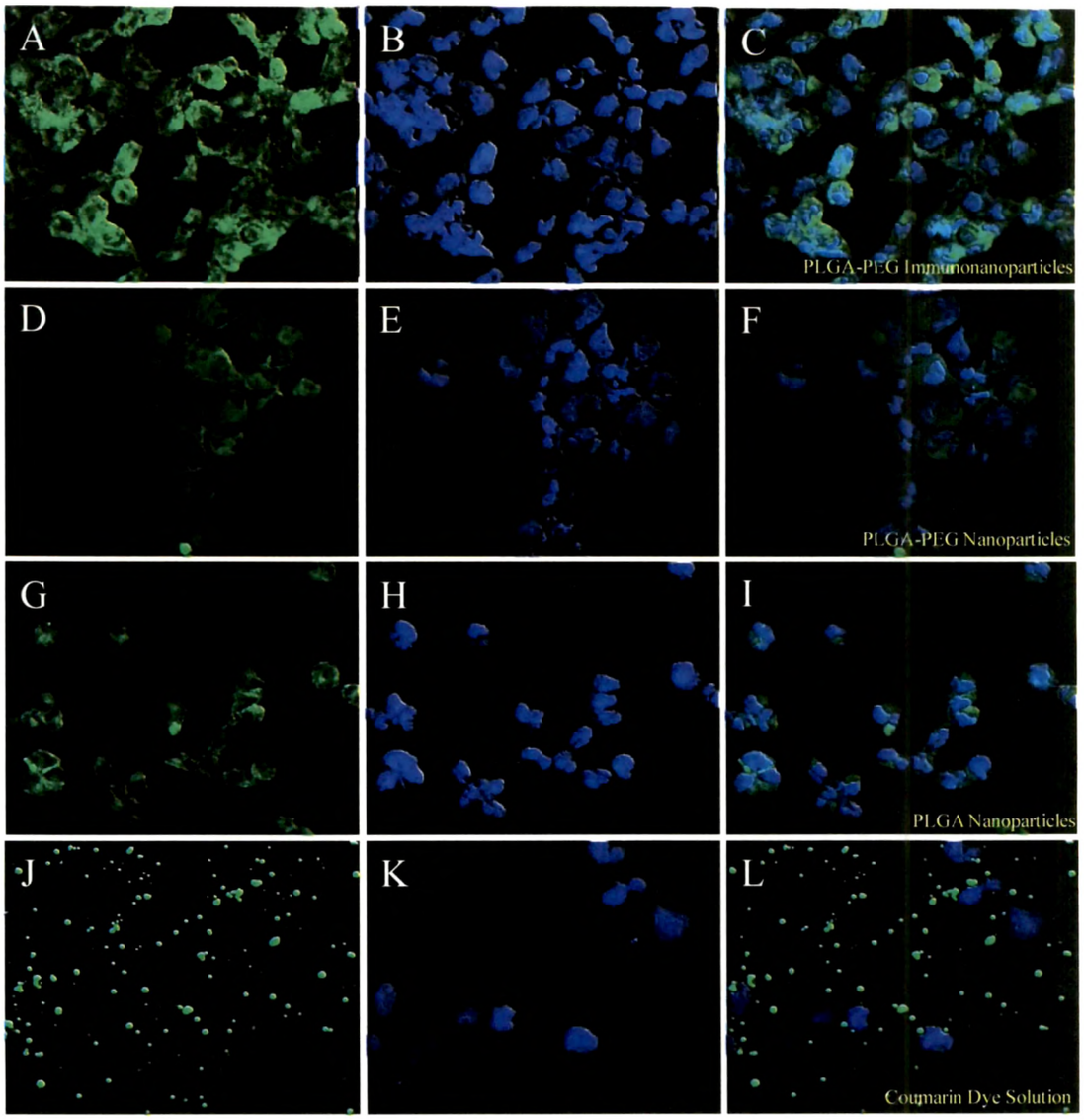

Figure 6.7 Qualitative cellular uptake of PLGA NPs, pegylated PLGA and ImmunoNPs using fluorescent microscope. (A-C) ImmunoNPs; (D-F) pegylated PLGA NPs; (G-I) PLGA NPs; (J-L) 6-Coumarin dye solution; (B, E, H and K) nucleus stained using Hoechst 33342; (C, F, I and L) overlapping images.

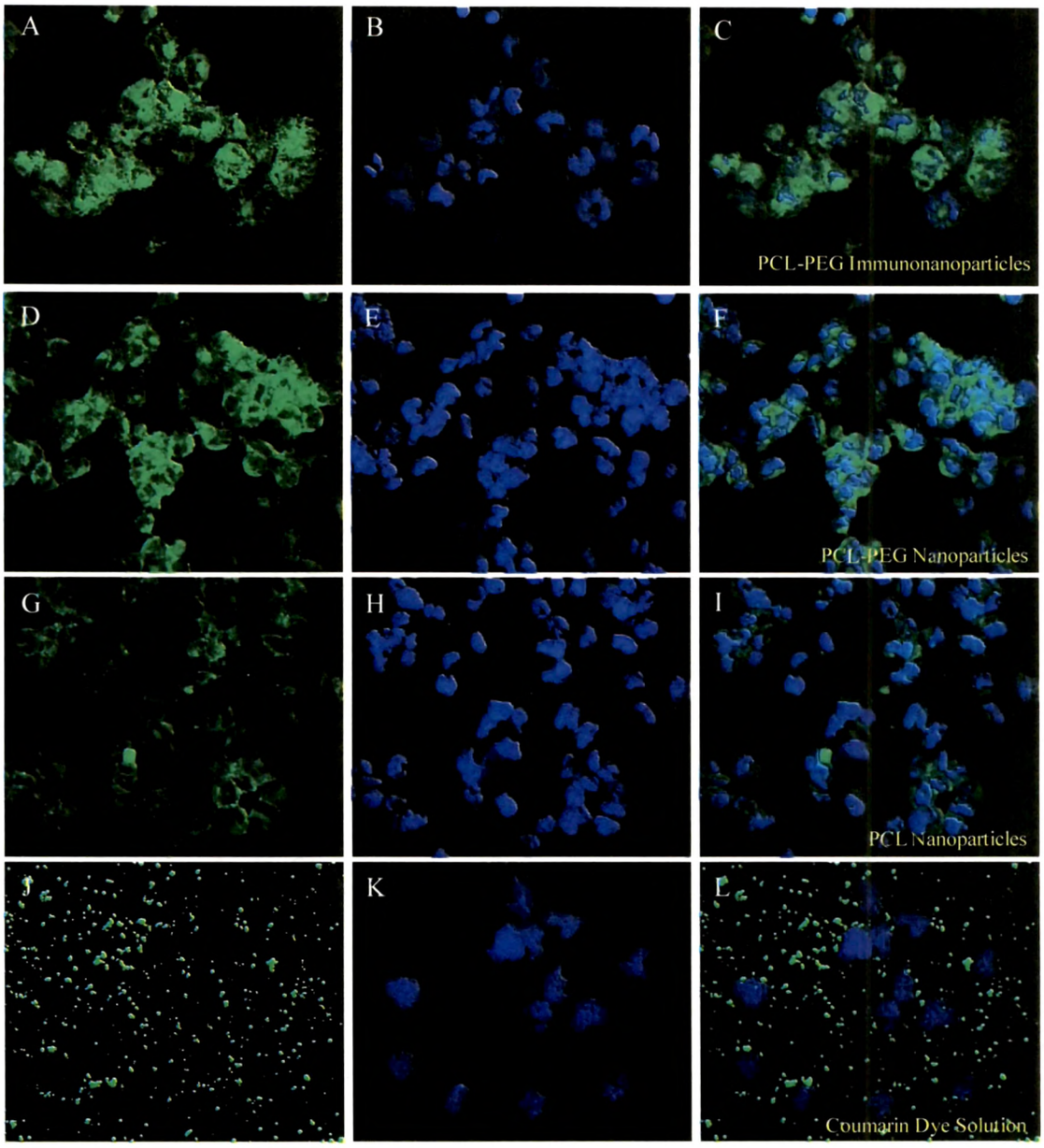

Figure 6.8 Qualitative cellular uptake of PCL NPs, pegylated PCL NPs and ImmunoNPs using fluorescent microscope. (A-C) ImmunoNPs; (D-F) pegylated PCL NPs; (G-I) PCL NPs; (J-L) 6-Coumarin dye solution; (B, E, H and K) nucleus stained using Hoechst 33342; (C, F, I and L) overlapping images.

6.5.3 In vitro cytotoxicity studies by MTT Assay

In vitro cytotoxicity studies were performed on ER positive (MCF7) as well as ER negative (MDAMB231) cell line by MTT assay and it demonstrated that ER antibody conjugated NPs showed higher anti-proliferative effect than un-conjugated NPs at all concentrations and at all time points in MCF7 cells. Cytotoxicity curve and IC_{50} value

were determined for ATZ, ATZ PLGA NPs, ATZ PLGA-PEG NPs and ATZ PLGA-PEG ImmunoNPs (figure 6.9, table 6.3). Blank Pegylated PLGA NPs (without ATZ) were also evaluated for cytotoxicity and found to be non-toxic. The IC_{50} value for ER positive cells treated with PLGA-PEG ImmunoNPs was found to be 163.65, 51.93 and 27.69 times lower than ATZ, ATZ PLGA NPs, ATZ PLGA-PEG NPs respectively, after 6 h of treatment. Exposure for 48 h further lowered the IC_{50} value by 3.6 times to 0.08 μM which was 8.25 times less in comparison with ATZ PLGA-PEG NPs. The enhanced cytotoxic effect of ATZ PLGA-PEG ImmunoNPs could be attributed to higher uptake via receptor mediated endocytosis. To confirm receptor mediated endocytosis, cytotoxicity studies were also performed on receptor negative cells (MDAMB231) and results clearly indicated that the effect of different NPs on MDAMB231 cells when compared to MCF7 cells. No significant toxicity was found on MDAMB231 cells. Thus, the enhanced cytotoxic activity of PLGA-PEG ImmunoNPs for MCF7 cells as compared with MDAMB231 cells clearly demonstrates the high affinity of ImmunoNPs towards ER positive cancer cells. Moreover, pegylated NPs showed comparatively more cytotoxicity towards MDAMB231 cells than PLGA NPs which indicated the role of pegylation in improving the efficacy of the NPs due to presence of hydrophilic PEG chains on the NPs [Chaudhari et al. 2012c]. However, no significant difference in % viability of these ER negative cells was observed after exposure to ATZ PLGA-PEG NPs and PLGA-PEG ImmunoNPs.

In vitro cytotoxicity studies of ATZ, ATZ PCL NPs, ATZ PCL-PEG NPs and ATZ PCL-PEG ImmunoNPs were performed on ER positive (MCF7) as well as ER negative (MDAMB231) cell line and it demonstrated that ER antibody conjugated NPs showed higher anti-proliferative effect than un-conjugated NPs at all concentrations and at all time points in MCF7 cells. Cytotoxicity curve and IC_{50} value were determined and presented in figure 6.10 and table 6.3. Blank Pegylated PCL NPs (without ATZ) were also evaluated for cytotoxicity and found to be non-toxic. The IC_{50} value for ER positive cells treated with PCL-PEG ImmunoNPs was found to be 158.2, 26.73 and 4.27 times lower than ATZ, ATZ PCL NPs, PCL-PEG NPs respectively, after 6 h of treatment. Exposure for 48 h further lowered the IC_{50} value by 6 times to 0.05 μM which was more than 6.6 times less in comparison with ATZ PCL-PEG NPs. To confirm receptor mediated endocytosis, cytotoxicity studies were also performed on receptor negative

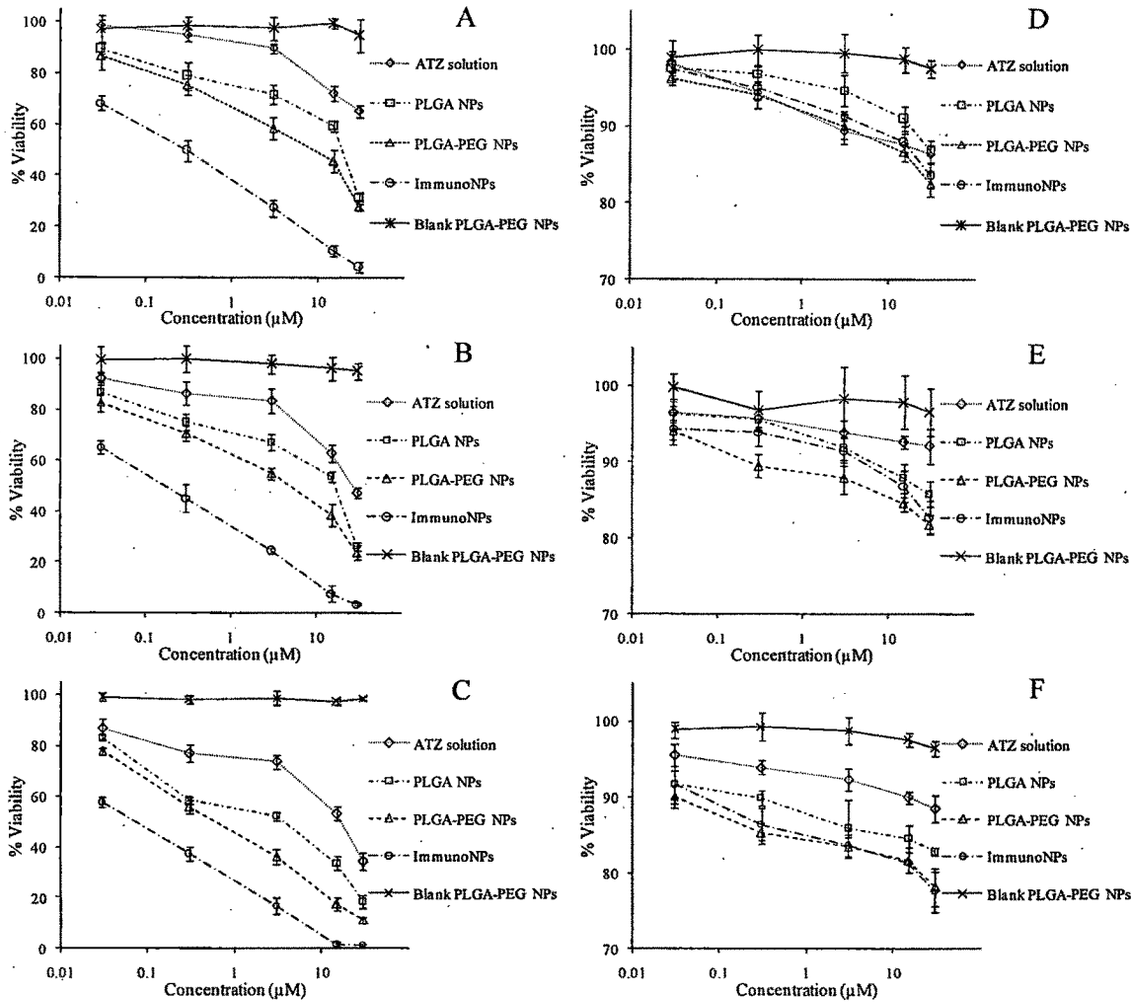

Figure 6.9 Cytotoxicity of ATZ loaded formulations (solution, PLGA NPs, PLGA-PEG NPs, ImmunoNPs) and blank PLGA-PEG NPs on MCF7 (A,B,C) and MDAMB231(D,E,F) cells after exposure for 6 h (A, D), 24 h (B, E) and 48 h (C, F).

cells (MDAMB231) and results clearly indicated that the effect of different NPs on MDAMB231 cells when compared to MCF7 cells. No significant toxicity was found on MDAMB231 cells. Thus, the enhanced cytotoxic activity of PCL-PEG ImmunoNPs for MCF7 cells as compared with MDAMB231 cells clearly demonstrates the high affinity of ImmunoNPs towards ER positive cancer cells. Moreover, pegylated NPs showed comparatively more cytotoxicity towards MDAMB231 cells than PCL NPs which indicated the role of pegylation in improving the efficacy of the NPs due to presence of hydrophilic PEG chains on the NPs [Chaudhari et al. 2012c]. However, no significant difference in % viability of these ER negative cells was observed after exposure to ATZ PCL-PEG NPs and PCL-PEG ImmunoNPs.

Table 6.3 Cytotoxicity of ATZ loaded formulations tested on MCF7 cell line (IC_{50} value)

	ATZ	ATZ PLGA NPs	ATZ PLGA-PEG NPs	ATZ PLGA-PEG ImmunoNPs	ATZ PCL NPs	ATZ PCL-PEG NPs	ATZ PCL-PEG ImmunoNPs
6 h	47.46	15.06	8.03	0.29	8.02	1.28	0.30
24 h	24.66	11.21	5.40	0.20	6.52	0.91	0.28
48 h	14.21	3.56	0.66	0.08	3.38	0.33	0.05

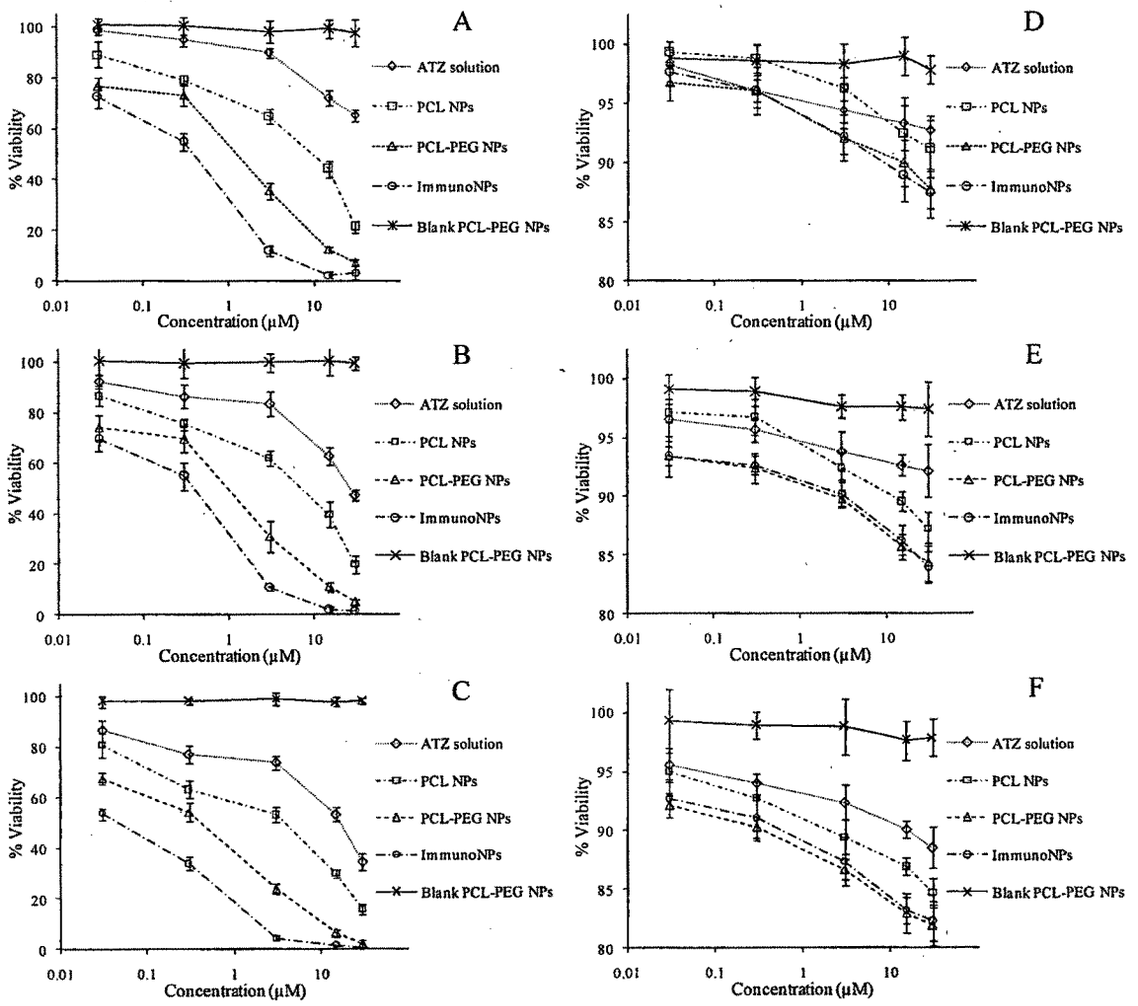

Figure 6.10 Cytotoxicity of ATZ loaded formulations (solution, PCL NPs, PCL-PEG NPs, ImmunoNPs) and blank PCL-PEG NPs on MCF7 (A,B,C) and MDAMB231 (D,E,F) cells after exposure for 6 h (A, D), 24 h (B, E) and 48 h (C, F).

In vitro cytotoxicity studies of EXE, EXE PLGA NPs, EXE PLGA-PEG NPs and EXE PLGA-PEG ImmunoNPs were performed on ER positive (MCF7) as well as ER negative (MDAMB231) cell line and it demonstrated that ER antibody conjugated NPs showed

higher anti-proliferative effect than un-conjugated NPs at all concentrations and at all time points in MCF7 cells. Cytotoxicity curve and IC_{50} value were determined and presented in figure 6.11 and table 6.4. Blank Pegylated PLGA NPs (without EXE) were also evaluated for cytotoxicity and found to be non-toxic. The IC_{50} value for ER positive cells treated with PLGA-PEG ImmunoNPs was found to be 7.5, 4.4 and 2.1 times lower than EXE, EXE PLGA NPs, EXE PLGA-PEG NPs respectively, after 48 h of treatment. To confirm receptor mediated endocytosis, cytotoxicity studies were also performed on receptor negative cells (MDAMB231) and results clearly indicated that the effect of different NPs on MDAMB231 cells when compared to MCF7 cells. No significant toxicity was found on MDAMB231 cells. Thus, the enhanced cytotoxic activity of EXE PLGA-PEG ImmunoNPs for MCF7 cells as compared with MDAMB231 cells clearly demonstrates the high affinity of ImmunoNPs towards ER positive cancer cells. Moreover, pegylated NPs showed comparatively more cytotoxicity towards MDAMB231 cells than EXE PLGA NPs which indicated the role of pegylation in improving the efficacy of the NPs due to presence of hydrophilic PEG chains on the NPs [Chaudhari et al. 2012c]. However, no significant difference in % viability of these ER negative cells was observed after exposure to EXE PLGA-PEG NPs and EXE PLGA-PEG ImmunoNPs

In vitro cytotoxicity studies of EXE, EXE PCL NPs, EXE PCL-PEG NPs and EXE PCL-PEG ImmunoNPs were performed on ER positive (MCF7) as well as ER negative (MDAMB231) cell line and it demonstrated that ER antibody conjugated NPs showed higher anti-proliferative effect than un-conjugated NPs at all concentrations and at all time points in MCF7 cells. Cytotoxicity curve and IC_{50} value were determined and presented in figure 6.12 and table 6.4. Blank Pegylated PCL NPs (without EXE) were also evaluated for cytotoxicity and found to be non-toxic. The IC_{50} value for ER positive cells treated with EXE PCL-PEG ImmunoNPs was found to be 7.7, 4.18 and 2.12 times lower than EXE, EXE PCL NPs, PCL-PEG NPs respectively, after 48 h of treatment. To confirm receptor mediated endocytosis, cytotoxicity studies were also performed on receptor negative cells (MDAMB231) and results clearly indicated that the effect of different NPs on MDAMB231 cells when compared to MCF7 cells. No significant toxicity was found on MDAMB231 cells. Thus, the enhanced cytotoxic activity of EXE PCL-PEG ImmunoNPs for MCF7 cells as compared with MDAMB231 cells clearly demonstrates the high affinity of ImmunoNPs towards ER positive cancer cells. Moreover, pegylated NPs showed comparatively more cytotoxicity towards MDAMB231 cells than PCL NPs which

indicated the role of pegylation in improving the efficacy of the NPs due to presence of hydrophilic PEG chains on the NPs [Chaudhari et al. 2012c]. However, no significant difference in % viability of these ER negative cells was observed after exposure to EXE PCL-PEG NPs and EXE PCL-PEG ImmunoNPs.

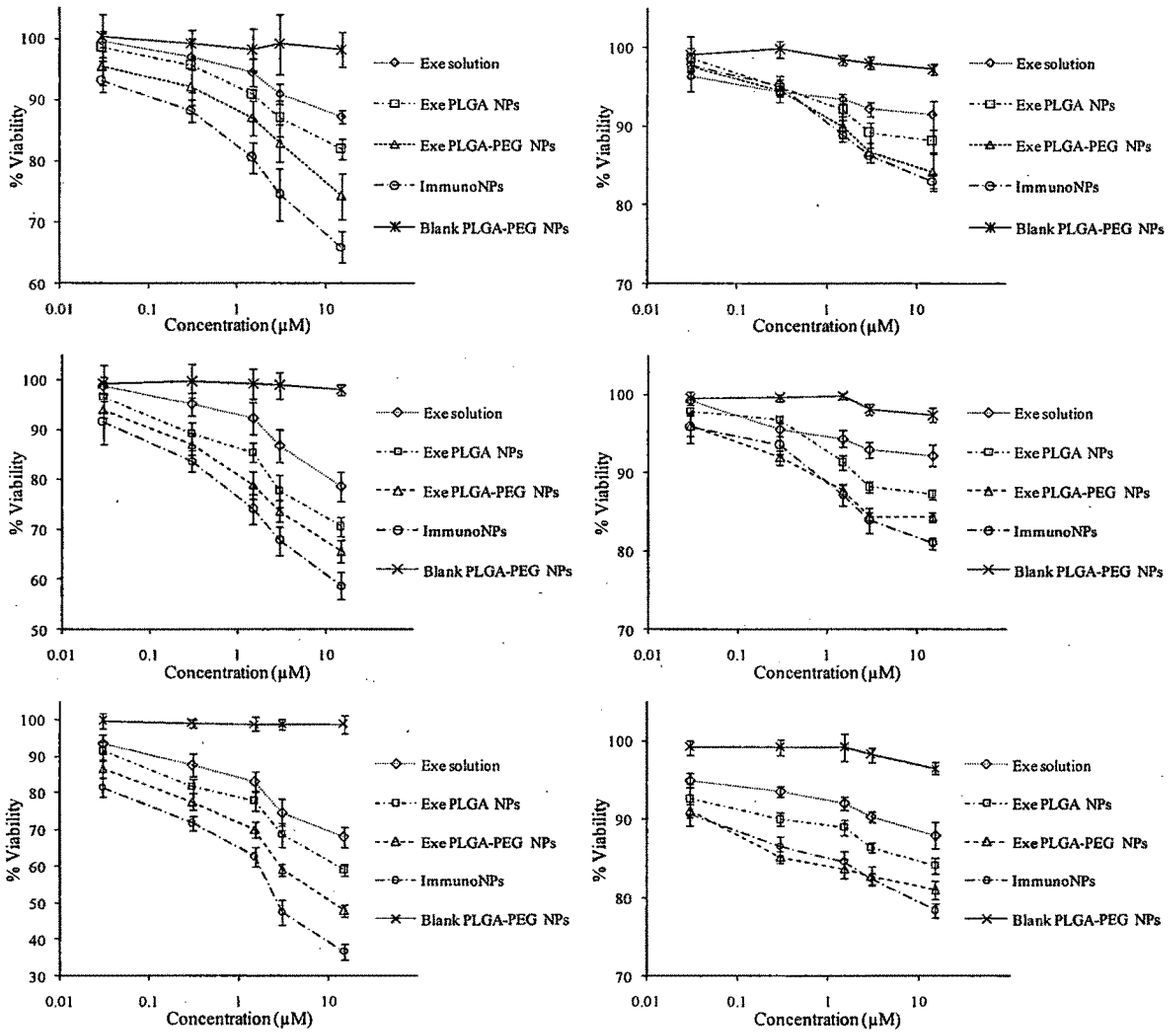

Figure 6.11 Cytotoxicity of EXE loaded formulations (solution, PLGA NPs, PLGA-PEG NPs, ImmunoNPs) and blank PLGA-PEG NPs on MCF7 (A,B,C) and MDAMB231 (D,E,F) cells after exposure for 6 h (A, D), 24 h (B, E) and 48 h (C, F).

Table 6.4 Cytotoxicity of EXE loaded formulations tested on MCF7 cell line (IC_{50} value)

	EXE	EXE PLGA NPs	EXE PLGA-PEG NPs	EXE PLGA-PEG ImmunoNPs	EXE PCL NPs	EXE PCL-PEG NPs	EXE PCL-PEG ImmunoNPs
6 h	28.84	18.24	11.21	6.44	15.21	9.68	6.27
24 h	15.5	8.66	6.14	3.86	8.61	6.19	3.84
48 h	7.24	4.20	1.96	0.96	3.93	1.99	0.94

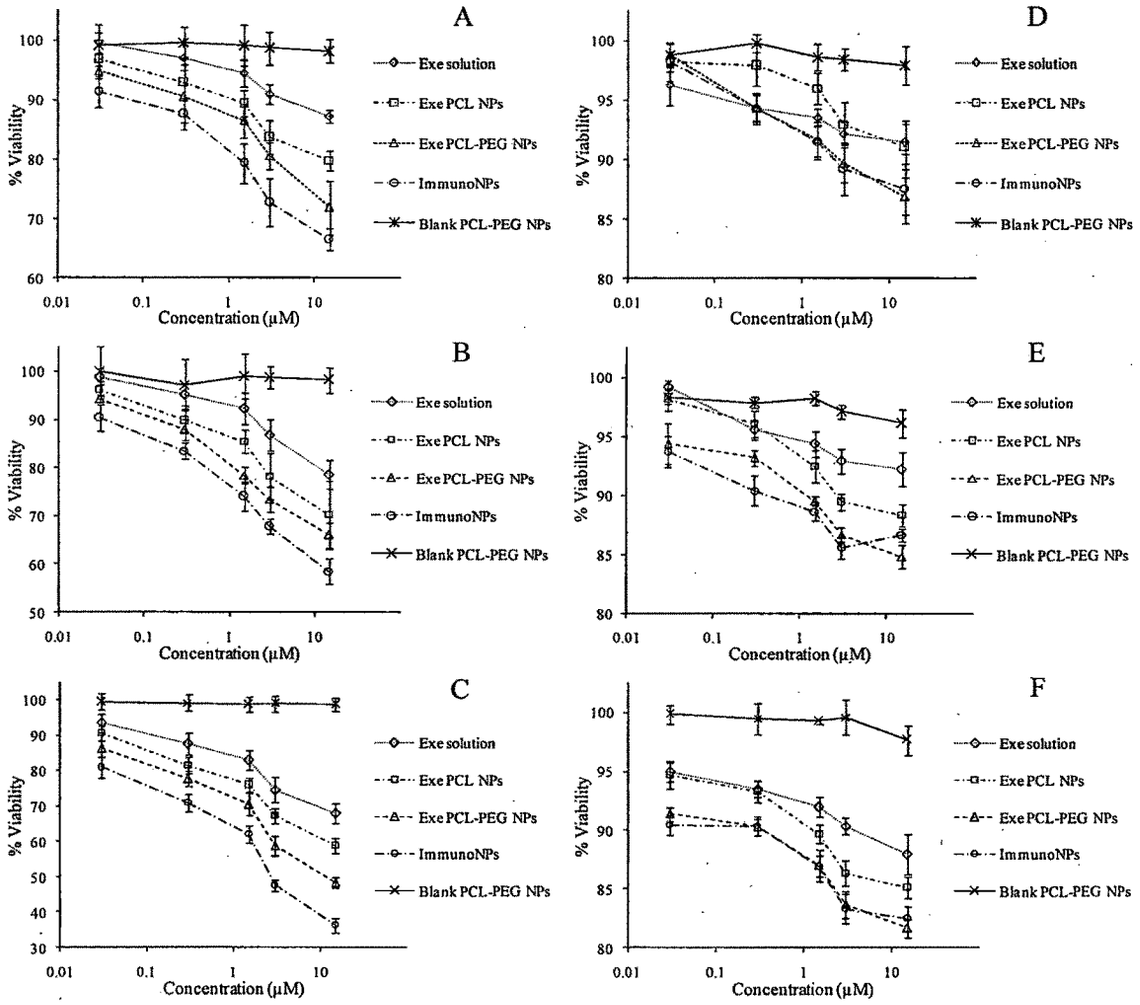

Figure 6 Cytotoxicity of Exe solution, Exe loaded PCL NPs, PCL-PEG NPs, ImmunoNPs and blank PCL-PEG NPs on MCF7 (A,B,C) and MDAMB231(D,E,F) cells after exposure for 6 h (A, D), 24 h (B, E) and 48 h (C, F).

Figure 6.12 Cytotoxicity of EXE loaded formulations (solution, PCL NPs, PCL-PEG NPs, ImmunoNPs) and blank PCL-PEG NPs on MCF7 (A,B,C) and MDAMB231 (D,E,F) cells after exposure for 6 h (A, D), 24 h (B, E) and 48 h (C, F).

6.5.4 Apoptosis studies

Apoptosis studies were carried out using annexin V procedure to determine whether drug loaded NPs caused apoptosis or necrosis of MCF7 cells. The membrane phospholipid, phosphatidylserine is translocated from the inner cytoplasm of the plasma membrane to the outer cell surface soon after the induction of apoptosis, and annexin V protein has a strong, specific affinity for phosphatidylserine, while the membranes of dead and damaged cells are permeable to propidium iodide and allows identifying the late apoptotic cells and necrotic populations. The results showed significant fraction of necrotic, early and late apoptotic population of cells after

exposure with ATZ drug solution, ATZ loaded PLGA NPs, PLGA-PEG NPs and PLGA-PEG ImmunoNPs. Control group treated with PBS showed only 1.6% and 3.6% cells in apoptotic phases after 24 and 48 h respectively. After 24 h of exposure with ATZ drug solution only 5.4% cells were in apoptotic phase (early and late apoptosis) whereas exposure with ATZ PLGA NPs, PLGA-PEG NPs and PLGA-PEG ImmunoNPs showed 32.6%, 43.7% and 60.9% cells in apoptotic phase which increased to 37.3%, 50.5% and 56.4%, respectively (figure 6.13, table 6.5). After 24 h of exposure with ATZ PCL NPs, PCL-PEG NPs and PCL-PEG ImmunoNPs showed 8%, 18% and 23.2% cells in apoptotic phase which increased to 12%, 34.7% and 53.8% after 48 h respectively (figure 6.14, table 6.6). With increase in exposure time to 48 h, the percentage of cells in early apoptotic phase decreased, at the same time percentage of cells in late apoptotic phase were found to be increased. This is possibly due to conversion of early apoptotic phase into late apoptotic phase. Similarly, percentage of cells undergone necrosis also increased with time but in less proportion than apoptosis indicating apoptosis as the possible mode of cell death. The augmented apoptotic activity of ImmunoNPs in comparison to ATZ drug solution and un-conjugated NPs can be correlated with the results of quantitative uptake showing higher endocytosis. Apoptotic signals were possibly activated by ImmunoNPs at very low concentration than drug solution or un-conjugated NPs. Targeted drug delivery showed enhanced apoptosis due to receptor mediated endocytosis which resulted in higher concentration of drug available for action at target site [Chaudhari et al. 2012b; Chaudhari et al. 2012c]. Sustained cytoplasmic delivery of ATZ from NPs coupled with ER antibody resulted in more enhanced therapeutic potency of the NPs by apoptosis than un-conjugated NPs or drug solution. Thus, ImmunoNPs were able to cause significant increase in programmed cell death when compared with ATZ drug solution or un-conjugated nanoparticulate preparations, thus supporting the hypothesis that ER antibody conjugated ImmunoNPs can serve as an effective delivery system for breast tumor targeting [Chaudhari et al. 2012b; Chaudhari et al. 2012c].

The results showed significant fraction of necrotic, early and late apoptotic population of cells after exposure with EXE solution, EXE loaded PLGA NPs, PLGA-PEG NPs and PLGA-PEG ImmunoNPs. Control group treated with PBS showed only 0.2% and 0.4% cells in apoptotic phases. After 24 h of exposure, EXE PLGA NPs, PLGA-PEG NPs and PLGA-PEG ImmunoNPs showed 13.0%, 26.5% and 36.6% cells in apoptotic phase which

Table 6.5 Apoptosis studies in MCF7 cell line after treatment of (a) Control (PBS), (b) ATZ solution, ATZ loaded (c) PLGA, (d) PLGA-PEG and (d) PLGA-PEG ImmunoNPs using FACS technique.

Treatment	24 h				48 h			
	Q1	Q2	Q3	Q4	Q1	Q2	Q3	Q4
Control	0.0	0.6	98.4	1.0	0.2	3.1	96.1	0.5
ATZ solution	1.0	3.9	93.5	1.5	1.7	5.3	92.3	0.7
PLGA NPs	2.2	21.4	65.2	11.2	2.6	25.6	60.1	11.7
PLGA-PEG NPs	3.4	37.8	52.9	5.9	2.0	48.0	47.5	2.5
PLGA-PEG ImmunoNPs	3.2	48.9	35.9	12.0	5.4	56.3	38.1	0.1

Table 6.6 Apoptosis studies in MCF7 cell line after treatment of (a) Control (PBS), (b) ATZ solution, ATZ loaded (c) PCL, (d) PCL-PEG and (d) PCL-PEG ImmunoNPs using FACS technique.

Treatment	24 h				48 h			
	Q1	Q2	Q3	Q4	Q1	Q2	Q3	Q4
Control	0.0	0.6	98.4	1.0	0.2	3.1	96.1	0.5
ATZ solution	1.0	3.9	93.5	1.5	1.7	5.3	92.3	0.7
PCL NPs	3.1	5.5	88.8	2.5	5.5	11.7	75.3	0.3
PCL-PEG NPs	6.7	17.7	75.3	0.3	7.8	33.8	57.5	0.9
PCL-PEG ImmunoNPs	12.3	22.9	64.4	0.3	1.4	44.9	44.8	8.9

increased to 17.3%, 42.3% and 67.5%, respectively (figure 6.15, table 6.7). After 24 h of exposure with EXE PCL NPs, PCL-PEG NPs and PCL-PEG ImmunoNPs showed 9.8%, 25.7% and 35.4% cells in apoptotic phase which increased to 16.6%, 41.6% and 70.2% after 48 h respectively (figure 6.16, table 6.8). With increase in exposure time to 48 h, the percentage of cells in early apoptotic phase decreased, at the same time percentage of cells in late apoptotic phase were found to be increased. This is possibly due to conversion of early apoptotic phase into late apoptotic phase. Similarly, percentage of cells undergone necrosis also increased with time but in less proportion than apoptosis indicating apoptosis as the possible mode of cell death. The augmented apoptotic activity of ImmunoNPs in comparison to EXE drug solution and un-conjugated NPs can be correlated with the results of quantitative uptake showing higher endocytosis.

Apoptotic signals were possibly activated by ImmunoNPs at very low concentration than drug solution or un-conjugated NPs. Targeted drug delivery showed enhanced apoptosis due to receptor mediated endocytosis which resulted in higher concentration of drug available for action at target site [Chaudhari et al. 2012b; Chaudhari et al. 2012c]. Sustained cytoplasmic delivery of EXE from NPs coupled with ER antibody resulted in more enhanced therapeutic potency of the NPs by apoptosis than un-conjugated NPs or drug solution. Thus, ImmunoNPs were able to cause significant increase in programmed cell death when compared with EXE drug solution or un-conjugated nanoparticulate preparations, thus supporting the hypothesis that ER antibody conjugated ImmunoNPs can serve as an effective delivery system for breast tumor targeting [Chaudhari et al. 2012b; Chaudhari et al. 2012c].

Table 6.7 Apoptosis studies in MCF7 cell line after treatment of (a) Control (PBS), (b) EXE solution, EXE loaded (c) PLGA, (d) PLGA-PEG and (d) PLGA-PEG ImmunoNPs using FACS technique.

Treatment	24 h				48 h			
	Q1	Q2	Q3	Q4	Q1	Q2	Q3	Q4
Control	0.1	0.2	99.7	0.0	0.2	0.4	99.3	0.0
EXE solution	2.9	0.6	96.4	0.0	6.3	0.3	93.3	0.0
PLGA NPs	4.5	9.7	82.5	3.3	7.8	13.8	74.9	3.5
PLGA-PEG NPs	4.0	14.7	69.6	11.8	1.5	22.1	56.2	20.2
PLGA-PEG ImmunoNPs	0.9	22.3	62.4	14.3	0.3	39.5	32.2	28.0

Table 6.8 Apoptosis studies in MCF7 cell line after treatment of (a) Control (PBS), (b) EXE solution, EXE loaded (c) PCL, (d) PCL-PEG and (d) PCL-PEG ImmunoNPs using FACS technique.

Treatment	24 h				48 h			
	Q1	Q2	Q3	Q4	Q1	Q2	Q3	Q4
Control	0.1	0.2	99.7	0.0	0.2	0.4	99.3	0.0
EXE solution	2.9	0.6	96.4	0.0	6.3	0.3	93.3	0.0
PCL NPs	3.9	7.2	86.3	2.6	6.9	12.5	76.5	4.1
PCL-PEG NPs	3.1	14.2	71.2	11.5	2.4	21.6	55.9	20.0
PCL-PEG ImmunoNPs	1.6	21.4	63.1	14.0	0.5	44.8	29.3	25.4

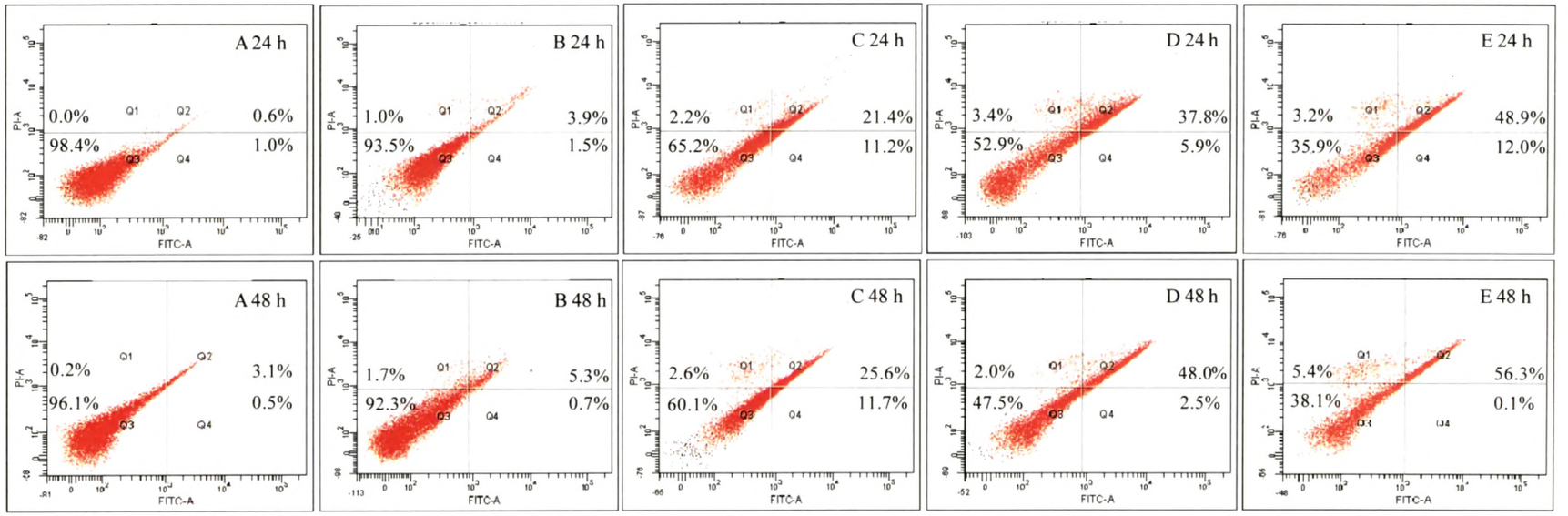

Figure 6.13 Apoptosis estimation in MCF7 cell line after exposure of Control (PBS), A; ATZ Solution, B; ATZ PLGA NPs, C; ATZ PLGA-PEG NPs, D; and ATZ PLGA-PEG ImmunoNPs, E; for 24 and 48 h by Annexin V-FITC and PI staining using FACS technique. Necrotic cells FITC (-) PI (+), Late apoptosis FITC (+) PI (+), Live FITC (-) PI (-), Early apoptotis FITC (+) PI (-).

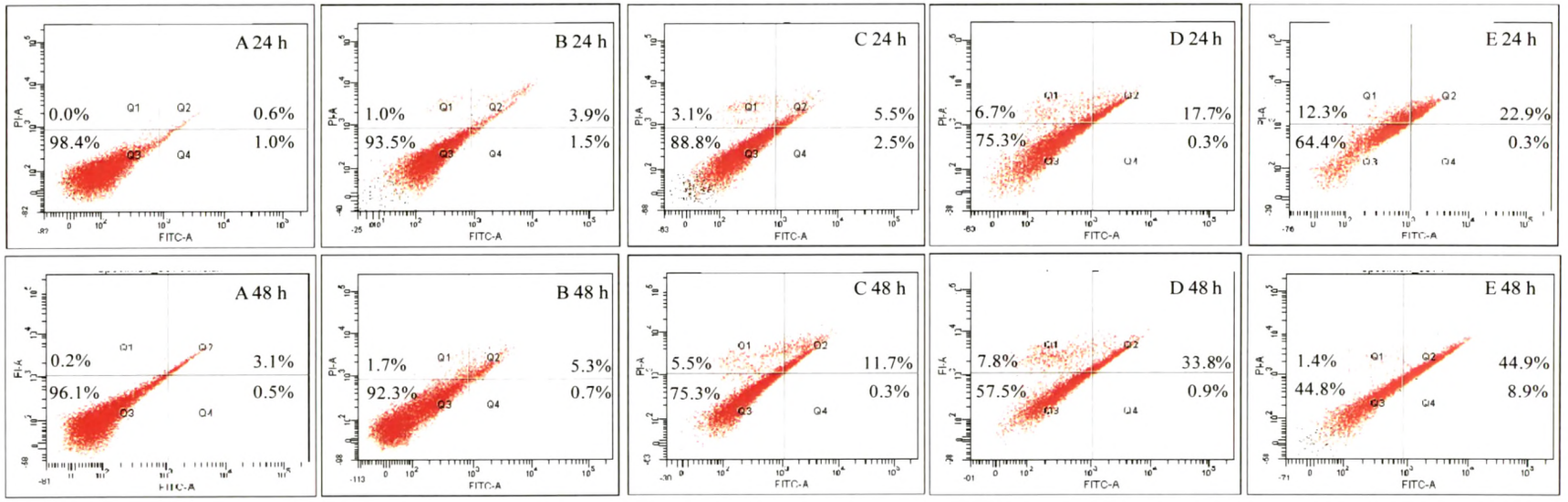

Figure 6.14 Apoptosis estimation in MCF7 cell line after exposure of Control (PBS), A; ATZ Solution, B; ATZ PCL NPs, C; ATZ PCL-PEG NPs, D; and ATZ PCL-PEG ImmunoNPs, E; for 24 and 48 h by Annexin V-FITC and PI staining using FACS technique. Necrotic cells FITC (-) PI (+), Late apoptosis FITC (+) PI (+), Live FITC (-) PI (-), Early apoptotis FITC (+) PI (-).

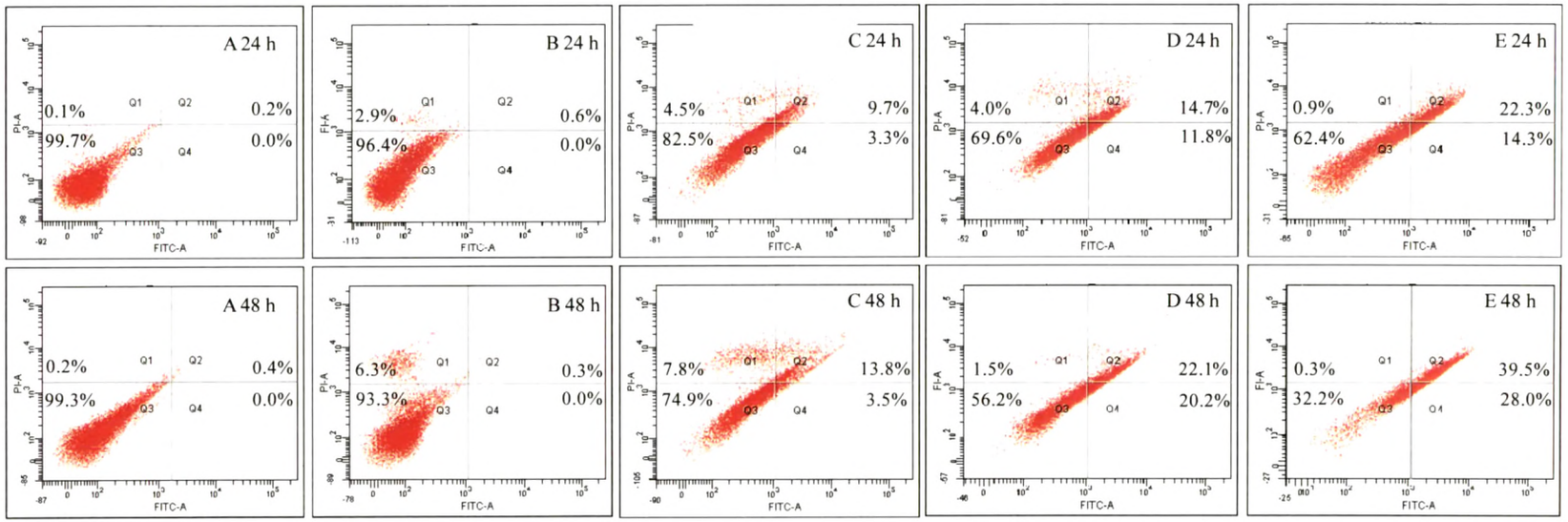

Figure 6.15 Apoptosis estimation in MCF7 cell line after exposure of Control (PBS), A; EXE Solution, B; EXE PLGA NPs, C; EXE PLGA-PEG NPs, D; and EXE PLGA-PEG ImmunoNPs, E; for 24 and 48 h by Annexin V-FITC and PI staining using FACS technique. Necrotic cells FITC (-) PI (+), Late apoptosis FITC (+) PI (+), Live FITC (-) PI (-), Early apoptotis FITC (+) PI (-).

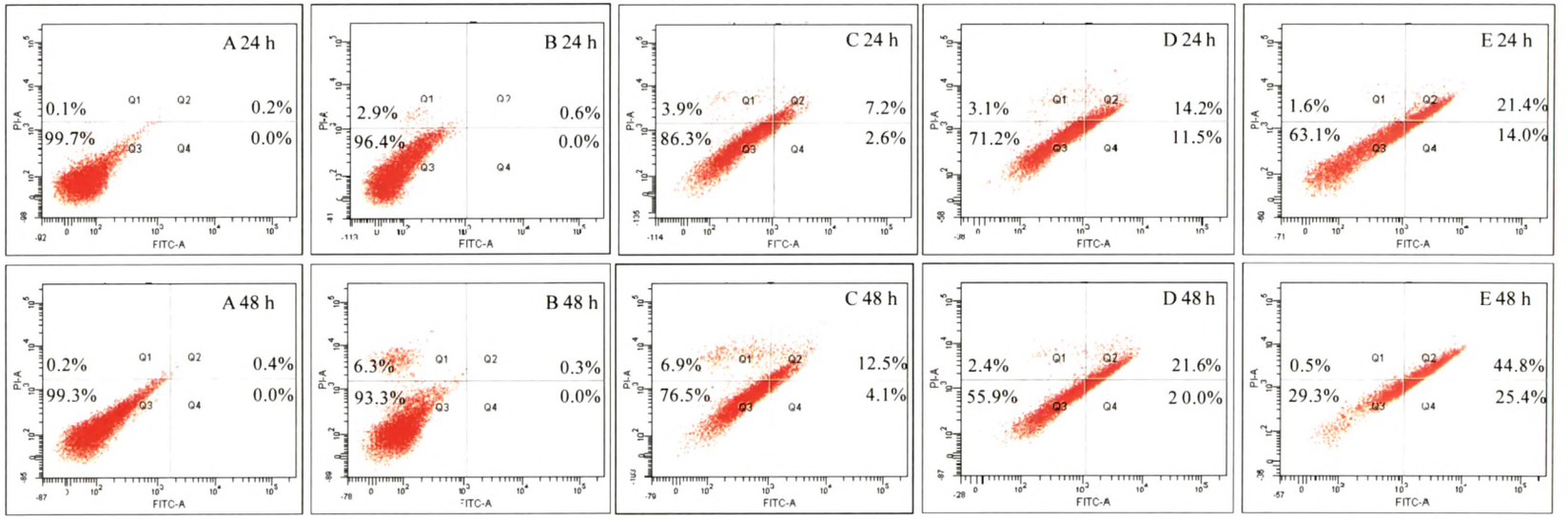

Figure 6.16 Apoptosis estimation in MCF7 cell line after exposure of Control (PBS), A; EXE Solution, B; EXE PCL NPs, C; EXE PCL-PEG NPs, D; and EXE PCL-PEG ImmunoNPs, E; for 24 and 48 h by Annexin V-FITC and PI staining using FACS technique. Necrotic cells FITC (-) PI (+), Late apoptosis FITC (+) PI (+), Live FITC (-) PI (-), Early apoptotis FITC (+) PI (-).

6.5.5 Cell cycle analysis

Drugs are known to act by different pharmacological actions which includes their effect on genes controlling the cell cycle and induction of pro- and anti-apoptotic genes [Panyam and Labhasetwar 2004]. Anastrozole is known to inhibit cell growth and proliferation primarily through apoptosis inducing mechanism and cell cycle arrest [Chaudhari et al. 2012a; Xanthopoulos et al. 2005] . Hence, we investigated whether the pharmacological action of anastrozole would affect the proliferation of breast cancer cells by studying the distribution of DNA in cell cycle. The DNA distribution in cell cycle was studied to investigate the effect of prepared formulations on growth of MCF7 cells. Results of cell cycle analysis demonstrated that ATZ treated cells showed stronger arrest at G0/G1 phase as compared to nanoparticulate formulations. ImmunoNPs showed lesser percentage of cells at G0/G1 phase (56.4%) as compared to 69.9% and 63.6% cells in PBS (control) and ATZ treated cells. However, exposure to ImmunoNPs showed stronger arrest at G2/M phase (27.1%) which was almost 1.6 times higher than ATZ drug solution (figure 6.17, table 6.9).

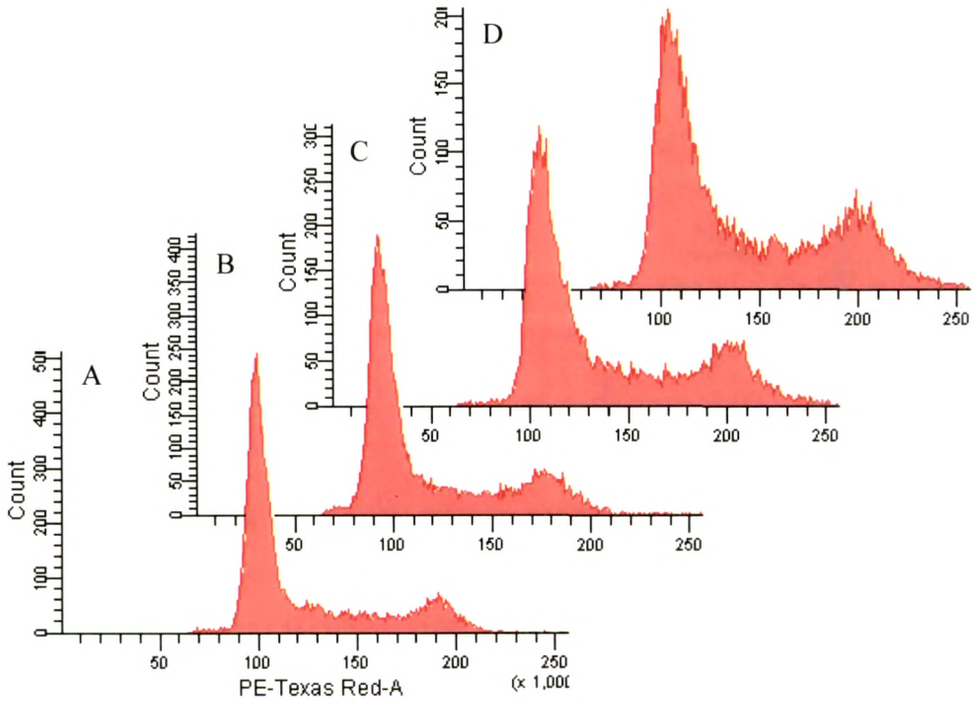

Figure 6.17 Effect of ATZ, ATZ loaded PLGA-PEG NPs and ImmunoNPs exposure on cell cycle distribution in MCF7 cells using FACS as an estimation technique.

Table 6.9 Cell cycle analysis in MCF7 cell line after treatment of (a) Control (PBS), (b) ATZ solution, ATZ loaded (c) PLGA-PEG NPs and (d) PLGA-PEG ImmunoNPs by PI staining using FACS technique.

Treatment	Phases			
	Sub G0/G1	G0/G1	S	G2/M
Control	1.4	69.9	12.7	16.0
ATZ solution	2.8	63.6	16.4	17.2
PLGA-PEG NPs	1.0	59.6	14.5	25.0
PLGA-PEG ImmunoNPs	0.9	56.4	15.6	27.1

Results of cell cycle analysis demonstrated that ATZ treated cells showed stronger arrest at G0/G1 phase as compared to nanoparticulate formulations. ImmunoNPs showed lesser percentage of cells at G0/G1 phase (50.1%) as compared to 69.9% and 63.6% cells in PBS (control) and ATZ treated cells. However, exposure to ImmunoNPs showed stronger arrest at G2/M phase (29.3%) which was almost 1.7 times higher than ATZ drug solution (figure 6.18, table 6.10).

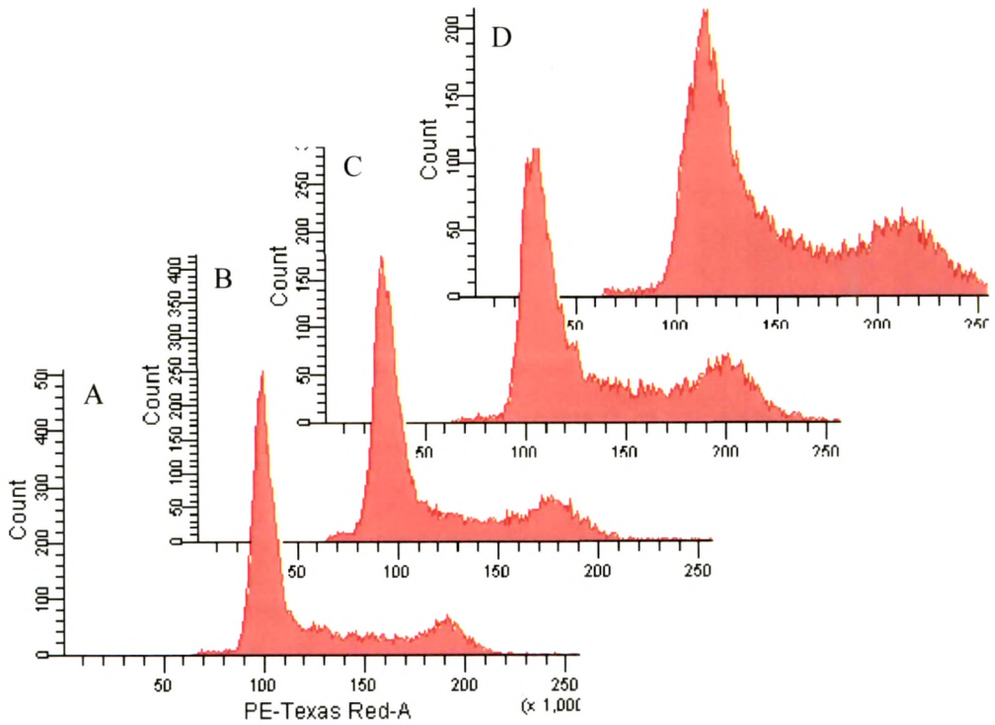

Figure 6.18 Effect of ATZ, ATZ loaded PCL-PEG NPs and ImmunoNPs exposure on cell cycle distribution in MCF7 cells using FACS as an estimation technique.

Table 6.10 Cell cycle analysis in MCF7 cell line after treatment of (a) Control (PBS), (b) ATZ solution, ATZ loaded (c) PCL-PEG NPs and (d) PCL-PEG ImmunoNPs by PI staining using FACS technique.

Treatment	Phases			
	Sub G0/G1	G0/G1	S	G2/M
Control	1.4	69.9	12.7	16.0
ATZ solution	2.8	63.6	16.4	17.2
PCL-PEG NPs	1.1	59.9	14.2	24.8
PCL-PEG ImmunoNPs	1.0	50.1	19.6	29.3

Results of cell cycle analysis demonstrated that EXE treated cells showed stronger arrest at G0/G1 phase as compared to nanoparticulate formulations. ImmunoNPs showed lesser percentage of cells at G0/G1 phase (48.2%) as compared to 68.6% and 60.2% cells in PBS (control) and EXE treated cells. However, exposure to ImmunoNPs showed stronger arrest at G2/M phase (28.5%) which was almost 1.33 times higher than EXE drug solution (figure 6.19, table 6.11).

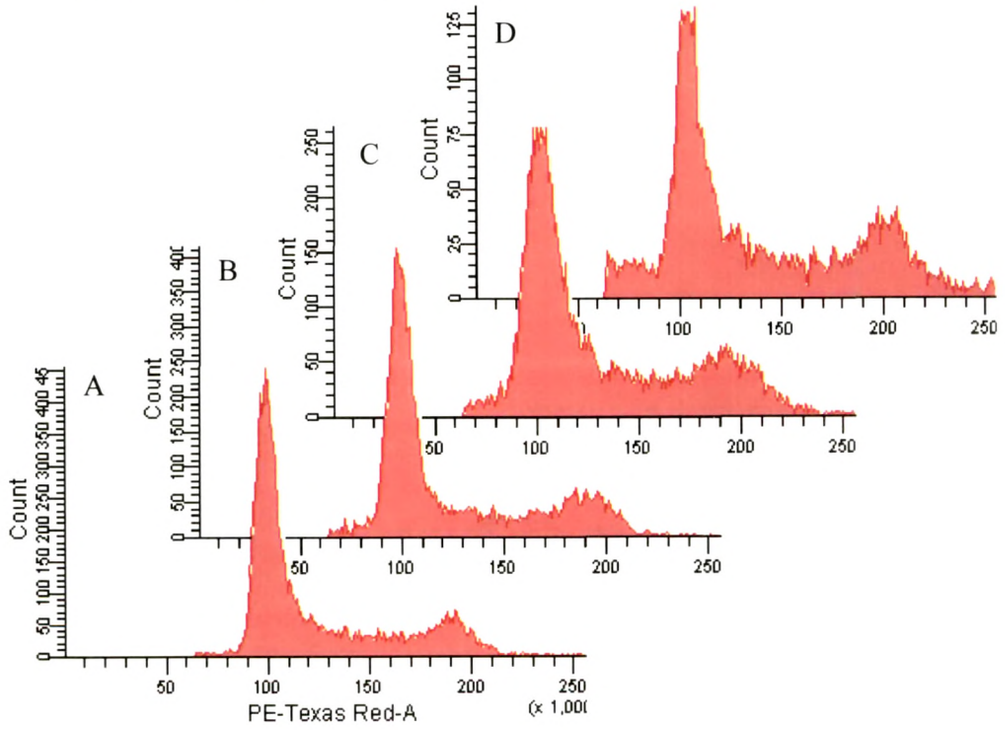

Figure 6.19 Effect of EXE, EXE loaded PLGA-PEG NPs and ImmunoNPs exposure on cell cycle distribution in MCF7 cells using FACS as an estimation technique.

Table 6.11 Cell cycle analysis in MCF7 cell line after treatment of (a) Control (PBS), (b) EXE solution, EXE loaded (c) PLGA-PEG NPs and (d) PLGA-PEG ImmunoNPs by PI staining using FACS technique.

Treatment	Phases			
	Sub G0/G1	G0/G1	S	G2/M
Control	1.5	68.6	13.1	16.8
EXE solution	2.4	60.2	15.9	21.4
PLGA-PEG NPs	2.9	53.3	19.8	24.0
PLGA-PEG ImmunoNPs	6.2	48.2	17.1	28.5

Results of cell cycle analysis demonstrated that EXE treated cells showed stronger arrest at G0/G1 phase as compared to nanoparticulate formulations. ImmunoNPs showed lesser percentage of cells at G0/G1 phase (45.3%) as compared to 68.6% and 60.2% cells in PBS (control) and EXE treated cells. However, exposure to ImmunoNPs showed stronger arrest at G2/M phase (34.2%) which was almost 1.6 times higher than EXE drug solution (figure 6.20, table 6.12).

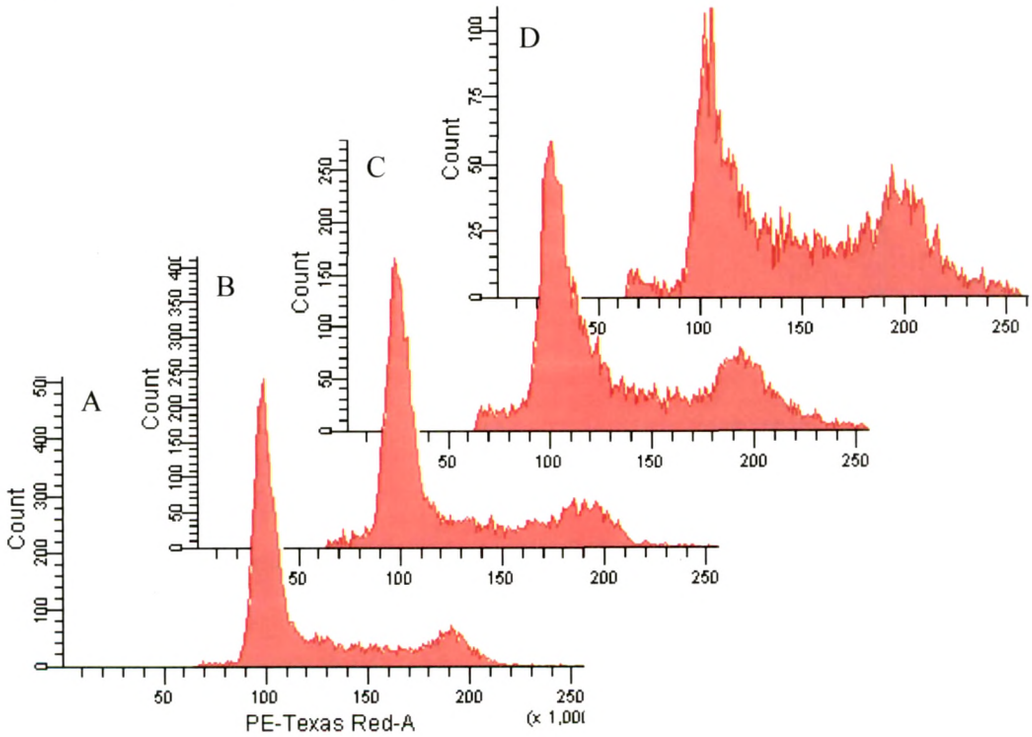

Figure 6.20 Effect of EXE, EXE loaded PCL-PEG NPs and ImmunoNPs exposure on cell cycle distribution in MCF7 cells using FACS as an estimation technique.

Table 6.12 Cell cycle analysis in MCF7 cell line after treatment of (a) Control (PBS), (b) EXE solution, EXE loaded (c) PCL-PEG NPs and (d) PCL-PEG ImmunoNPs by PI staining using FACS technique.

Treatment	Phases			
	Sub G0/G1	G0/G1	S	G2/M
Control	1.5	68.6	13.1	16.8
EXE solution	2.4	60.2	15.9	21.4
PCL-PEG NPs	4.0	56.9	13.2	25.9
PCL-PEG ImmunoNPs	2.6	45.3	17.9	34.2

Previously, it was observed by Chaudhari et al. that ligand conjugated NPs were more effective in controlling cell cycle arrest as compared to drug solution in MCF7 cells [Chaudhari et al. 2012a; Chaudhari et al. 2012b; Chaudhari et al. 2012c]. Our results suggested that higher anti-proliferative effects of ImmunoNPs on MCF7 cells may be due to decreased cell cycle progression. However, greater efficiency of ImmunoNPs in arresting more number of cells depends on the intracellular drug level in the target cells due to enhanced cellular uptake following receptor mediated endocytosis and sustained drug release as compared to drug solution and un-conjugated NPs.

6.6 References

Bareford LM, Swaan PW. 2007. Endocytic mechanisms for targeted drug delivery. Adv. Drug Deliv. Rev. 59(8):748-758.

Bradford MM. 1976. A rapid and sensitive method for the quantitation of microgram quantities of protein utilizing the principle of protein-dye binding. Anal. Biochem. 72:248-254.

Castino R, Démoz M, Isidoro C. 2003. Destination 'Lysosome': a target organelle for tumour cell killing? J. Mol. Recog. 16(5):337-348.

Chaudhari KR, Kumar A, Khandelwal VKM, Mishra AK, Monkkonen J, Murthy RSR. 2012a. Targeting efficiency and biodistribution of zoledronate conjugated docetaxel loaded pegylated PBCA nanoparticles for bone metastasis. Adv. Func. Mat. 22(19):4101-4114.

Chaudhari KR, Kumar A, Khandelwal VKM, Ukawala M, Manjappa AS, Mishra AK, Monkkonen J, Murthy RSR. 2012b. Bone metastasis targeting: A novel approach

to reach bone using Zoledronate anchored PLGA nanoparticle as carrier system loaded with Docetaxel. J. Controlled Rel. 158(3):470-478.

Chaudhari KR, Ukawala M, Manjappa AS, Kumar A, Mundada PK, Mishra AK, Mathur R, Monkkonen J, Murthy RS. 2012c. Opsonization, biodistribution, cellular uptake and apoptosis study of PEGylated PBCA nanoparticle as potential drug delivery carrier. Pharm. Res. 29(1):53-68.

Loveland BE, Johns TG, Mackay IR, Vaillant F, Wang ZX, Hertzog PJ. 1992. Validation of the MTT dye assay for enumeration of cells in proliferative and antiproliferative assays. Biochem. Int. 27(3):501-510.

Mosmann T. 1983. Rapid colorimetric assay for cellular growth and survival: application to proliferation and cytotoxicity assays. J. Immunol. Methods 65(1-2):55-63.

Panyam J, Labhasetwar V. 2003. Dynamics of endocytosis and exocytosis of poly(D,L-lactide-co-glycolide) nanoparticles in vascular smooth muscle cells. Pharm. Res. 20(2):212-220.

Panyam J, Labhasetwar V. 2004. Sustained cytoplasmic delivery of drugs with intracellular receptors using biodegradable nanoparticles. Mol. Pharm. 1(1):77-84.

Sahoo SK, Labhasetwar V. 2005. Enhanced antiproliferative activity of transferrin-conjugated paclitaxel-loaded nanoparticles is mediated via sustained intracellular drug retention. Mol. Pharm. 2(5):373-383.

Sieuwerts AM, Klijn JG, Peters HA, Foekens JA. 1995. The MTT tetrazolium salt assay scrutinized: how to use this assay reliably to measure metabolic activity of cell cultures in vitro for the assessment of growth characteristics, IC50-values and cell survival. Eur. J. Clin. Chem. Clin. Biochem. 33(11):813-823.

Sly WS, Vogler C. 2002. Brain-directed gene therapy for lysosomal storage disease: going well beyond the blood- brain barrier. Proc. Natl. Acad. Sci. USA 99(9):5760-5762.

Susin SA, Daugas E, Ravagnan L, Samejima K, Zamzami N, Loeffler M, Costantini P, Ferri KF, Irinopoulou T, Prevost MC and others. 2000. Two distinct pathways leading to nuclear apoptosis. J. Exp. Med. 192(4):571-580.

Van Maerken T, Speleman F, Vermeulen J, Lambertz I, De Clercq S, De Smet E, Yigit N, Coppens V, Philippe J, De Paepe A and others. 2006. Small-molecule MDM2

antagonists as a new therapy concept for neuroblastoma. Cancer Res. 66(19):9646-9655.

Vega F, Medeiros LJ, Leventaki V, Atwell C, Cho-Vega JH, Tian L, Claret FX, Rassidakis GZ. 2006. Activation of mammalian target of rapamycin signaling pathway contributes to tumor cell survival in anaplastic lymphoma kinase-positive anaplastic large cell lymphoma. Cancer Res. 66(13):6589-6597.

Xanthopoulos JM, Romano AE, Majumdar SK. 2005. Response of mouse breast cancer cells to anastrozole, tamoxifen, and the combination. J. Biomed. Biotechnol. 2005(1):10-19.